# Nonequilibrium clustering of self-propelled rods

Fernando Peruani, Andreas Deutsch, Markus Baer

# Non-equilibrium clustering of self-propelled rods

Fernando Peruani,[1,2] Andreas Deutsch,[2] and Markus Bär[3]

[1] *Max Planck Institute for Physics of Complex Systems, Nöthnitzer Str. 38, 01187 Dresden, Germany*
[2] *ZIH, TU Dresden, Zellescher Weg 12, 01069 Dresden, Germany*
[3] *Physikalisch-Technische Bundesanstalt, Abbestr. 2-12, 10587 Berlin, Germany*

(Dated: February 6, 2008)

Motivated by aggregation phenomena in gliding bacteria, we study collective motion in a two-dimensional model of active, self-propelled rods interacting through volume exclusion. In simulations with individual particles, we find that particle clustering is facilitated by a sufficiently large packing fraction $\eta$ or length-to-width ratio $\kappa$. The transition to clustering in simulations is well captured by a mean-field model for the cluster size distribution, which predicts that the transition values $\kappa_c$ of the aspect ratio for a fixed packing fraction $\eta$ is given by $\kappa_c = C/\eta - 1$ where $C$ is a constant.

PACS numbers: 87.18.Bb, 05.70.Ln, 87.18.Ed, 87.18.Hf

*Introduction.*— Emergent large-scale patterns of interacting self-driven motile elements are observed in a wide range of biological systems of different complexity: from human crowds, herds, bird flocks, and fish schools [1] to multicellular aggregates, e.g. of bacteria and amoebae [2] as well as sperms [3]. A recurrent question is how these entities coordinate their behavior to form groups which move collectively. At a theoretical level, several qualitative approaches have been made to incorporate the diverse collective behaviors of such different systems in a common framework [1, 4, 5]. More specific models for bacteria like *E. coli* as well as for amoebae like *D. discoideum* [2], have been based on chemotaxis, a long-range cell interaction mechanism according to which individual cells move in response to chemical signals produced by all other cells. However, in some bacteria there is no evidence for chemotactic cues and cells coordinate their movement by cell-to-cell signalling mechanisms in which physical contact between bacteria is needed [6]. Consequently, one may ask how such bacteria aggregate in order to communicate.

Another relevant aspect is the influence of the shape of the bacteria. The shape has been shown to be essential for individual motion of swimming bacteria [7]. In contrast, the role of the cell shape for collective motion has remained mostly unexplored. It has been demonstrated experimentally [8] that migrating elongated amoeboid cells exhibit alignment effects similar to those reported in liquid crystals [9]. A prominent example for collective behavior with no apparent long range interactions are the striking patterns observed during the life-cycle of gliding myxobacteria, see e.g. [6, 10]. Earlier modeling work has reproduced many of these patterns in three dimensions assuming either perfect alignment [11] or a phenomenological alignment force [12]. These models have all considered patterns resulting from exchange of chemical signals, that are absent in an early stage of the myxobacterial life cycle. Nevertheless, a trend from initial independent motion towards formation of larger clusters of aligned bacteria is often observed ( Fig. 1).

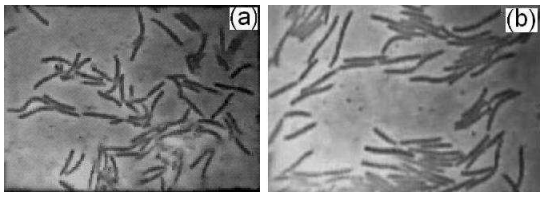


FIG. 1: Example for clustering of myxobacteria (*M. xanthus*) in the early stage of the life cycle. (a) Immediately after maturation of spores. (b) Afterwards, during the vegetative phase. Snapshots are taken from a movie (Ref. [10](b)), the frame size is 40 x 30 $\mu m^2$. Similar phenomena were seen in other bacterial species (*cf.* Ref. [6](a)).

Here, we study a model of self-propelled rods that have only repulsive excluded volume interactions in two dimensions. We find that the interplay of rod geometry, self-propulsion and repulsive short-range interaction is sufficient to facilitate aggregation into clusters. In simulations of an individual based model (IBM), clustering of self propelled particles (SPP) is observed for large enough packing fraction $\eta$ resp. aspect ratio $\kappa$ of the rods (see Fig. 2). We define the onset of clustering by the transition from a unimodal to a bimodal cluster size distribution. A mean-field approximation (MFA) for the cluster size distribution is derived and reproduces the change from a unimodal to a bimodal shape upon increase of either $\eta$ or $\kappa$. The MFA yields a simple equation $\kappa_c = C/\eta - 1$ for the critical rod aspect ratio, $\kappa_c$, at the onset of clustering in line with the IBM simulation results. fitted with $C = 1.46$. If diffusion is added to the active motion (active Brownian rods), the clustering transition is shifted to higher values of $\kappa$, whereas clustering is absent for pure diffusive motion (Brownian rods) as well as for isotropic particles with $\kappa = 1$. Hence, clustering of particles with excluded volume interaction requires both active motion, i. e. a non-equilibrium system, and elongated particles (= rods).

*Individual-based model (IBM).*— We consider $N$ rod-like particles moving on a plane. Each particle is

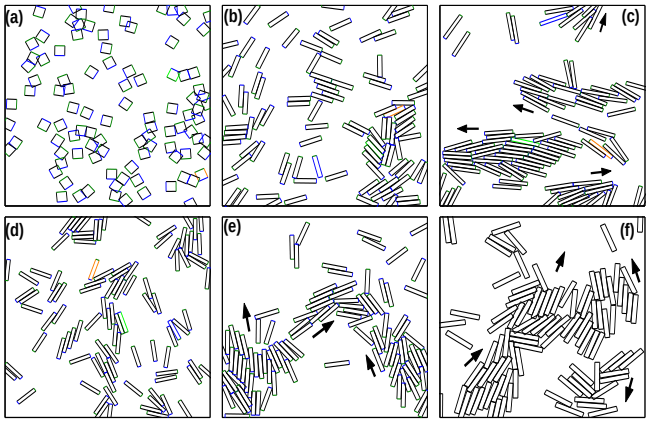


FIG. 2: Simulation snapshots of the steady states for different particle anisotropy $\kappa$ and the same packing fraction $\eta$ (a-c), and the same $\kappa$ and different $\eta$ (d-f). Fixing $\eta = 0.24$: (a) before the transition, $\kappa = 1$; (b) almost at the transition, $\kappa = 5$; (c) after the transition, $\kappa = 8$. Fixing $\kappa = 6$: (d) before the transition, $\eta = 0.18$; (e) just crossing the transition, $\eta = 0.24$; (f) after the transition, $\eta = 0.34$. In all cases, particles $N = 100$ and particle area $a = 0.2$. The arrows indicate the direction of motion of some of the clusters.

equipped with a self-propelling force acting along the long axis of the particle. We assume that particles are submerged in a viscous medium. Velocity and angular velocity are proportional to the force and torque, correspondingly. The rod-shape of the particles requires three different friction coefficients which correspond to the resistance exerted by the medium when particles either rotate or move along their long and short axes. Inertial terms are neglected (overdamped motion). Consequently the movement of the i-th rod is governed by the following equations for the velocity of its center of mass and angular velocity:

$$\begin{aligned}(v_{\parallel}^{(i)}, v_{\perp}^{(i)}) &= \left(\frac{1}{\zeta_{\parallel}}(F - \frac{\partial U^{(i)}}{\partial x_{\parallel}}), -\frac{1}{\zeta_{\perp}}\frac{\partial U^{(i)}}{\partial x_{\perp}}\right) \\ \dot{\theta}^{(i)} &= -\frac{1}{\zeta_{\theta}}\frac{\partial U^{(i)}}{\partial \theta} \end{aligned} \quad (1)$$

where $v_{\parallel}^{(i)}, v_{\perp}^{(i)}$ refer to the velocities along the long and short axis of the rods, respectively, $\zeta_i$ indicates the corresponding friction coefficients ($\zeta_\theta$ is related to the friction torque), $U^{(i)}$ refers to the energy of the interaction of the i-th rod with all other rods, and $F$ is the magnitude of the self-propelling force. The motion of the center of mass $\dot{\mathbf{x}}^{(i)} = (v_x^{(i)}, v_y^{(i)})$ of the i-th rod is given by

$$\begin{aligned} v_x^{(i)} &= v_{\parallel}^{(i)} \cos\theta^{(i)} + v_{\perp}^{(i)} \sin\theta^{(i)} \\ v_y^{(i)} &= v_{\parallel}^{(i)} \sin\theta^{(i)} - v_{\perp}^{(i)} \cos\theta^{(i)} \end{aligned} \quad (2)$$

Particles interact by ,,soft volume exclusion, *i. e.* by a potential that penalizes particle overlaps in the following way:

$$\begin{aligned} &U^{(i)}(\mathbf{x}^{(i)}, \theta^{(i)}, \mathbf{x}^{(j)}, \theta^{(j)}) \\ &= \phi \sum_{j=1, j\neq i}^{N} \left((\gamma - a_o(\mathbf{x}^{(i)}, \theta^{(i)}, \mathbf{x}^{(j)}, \theta^{(j)}))^{-\beta} - \gamma^{-\beta}\right) \end{aligned} \quad (3)$$

where $a_o(\mathbf{x}^{(i)}, \theta^{(i)}, \mathbf{x}^{(j)}, \theta^{(j)})$ is the area overlap of the rods $i$ and $j$, $\gamma$ is a parameter which can be associated to the maximum compressibility, $\beta$ controls the stiffness of the particle, and $\phi$ is the interaction strength. The simulations were performed placing $N$ identical particles initially at random inside a box of area $A$ with periodic boundary conditions. The values of the parameters are given in [13].

There are three key parameters which control the dynamics: i) persistence of particle motion, regulated by $F$, ii) the packing fraction $\eta$, i.e., the area occupied by rods divided by the total area ($\eta = Na/A$, where $N$ is the number of particles in the system, $a$ is the area of a single particle, and $A$ is the total area of the box), and iii) the length-to-width aspect ratio $\kappa$ ($\kappa = L/W$, where $L$ is the length and $W$ is the width of the rods). Simulations yield an increase of cluster formation with increasing $\kappa$ or $\eta$, see Fig. 2. Individual clusters are defined by connected particles that have non-zero overlap area. Simulations can be characterized by the mean maximum cluster size, $M$, and the weighted cluster size distribution, $p(m)$, which indicates the probability of finding a given particle inside a cluster of mass $m$. Fig. 3a shows that for a given $\eta$, $M$ seems to saturate after the critical $\kappa_c$ which is defined as the value of $\kappa$ for which the shape of $p(m)$ changes from unimodal to bimodal. In Fig. 3b typical shapes of $p(m)$ are shown: before clustering and corresponding to low values of $\kappa$ (circles), and after clustering and corresponding to large values of $\kappa$ (crosses). We define the onset of clustering by the emergence of a second peak in $p(m)$. We have also tested the robustness of the model against fluctuations by inserting additive noise terms $R_i/\zeta_i$ in Eqs. (1), which correspond to a switch from active to active Brownian particles [5]. We found that clustering is still present in rods of the latter kind, albeit the transition is moved to larger values of $\kappa$ and $\eta$. Clustering was absent in all simulations with purely Brownian rods ($F = 0$).

*Mean field approximation (MFA).*— We have studied the clustering effects described above through a MFA by deriving kinetic equations for the number $n_j$ of clusters of a given size $j$. The equations for $n_j$ contain terms for cluster fusion and fission. For the fusion terms we have adopted kinetic equations originally derived for coagulation of colloids [14], while the fission terms are empirically defined from the typical behavior seen in the above simulations. The numbers $n_j$ change in time - we have $\{n_j(t)\}_{j=1}^{\infty}$, where $n_j(t)$ is the number of clusters of mass $j$ at time $t$.

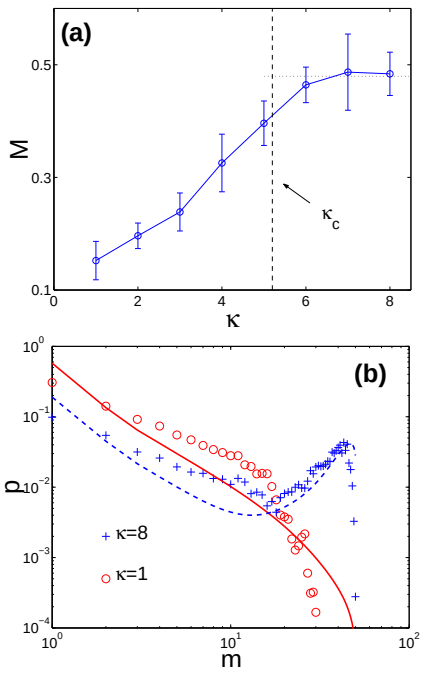


FIG. 3: (a) The mean maximum cluster size $M$ vs $\kappa$ for IBM simulations ($N = 50$). (b) $p(m)$ as function of the cluster size $m$ for $\eta = 0.34$. Symbols show the average over eight IBM simulations for active particles with $N = 50$ and $\kappa = 1$ (circles) and $\kappa = 8$ (crosses), errors bases give distributions of individual runs. The lines correspond to the mean field theory for $\kappa = 1$ (solid) and $\kappa = 8$ (dashed)(color online).

This description neglects the geometry of clusters as well as spatial fluctuations. This allows us to consider a single rate constant for all possible collision processes between clusters of mass $i$ and $j$, as well as a unique disintegration constant for any cluster of mass $i$. In addition we make four crucial assumptions: i) The total number of particles in the system, $N = \sum_{j=1}^{N} j n_j(t)$, is conserved. ii) Only binary cluster collisions are considered. Collisions between any two clusters are allowed whenever the sum of the cluster masses is less or equal to $N$. iii) Clusters suffer spontaneous fission only by losing individual particles at the boundary one by one, *i. e.* a cluster can only decay by a process by which a $j$-cluster split into a single particle plus a $(j-1)$-cluster. This is motivated by observations in the above simulations. iv) All clusters move at constant speed, $\widetilde{v} \approx F/\zeta_{\parallel}$, which implies that rods in a cluster have high orientational order and interact only very weakly with their neighbors. Under all these assumptions the evolution of the $n_j$'s is given by the following $N$ equations:

$$\dot{n}_1 = 2B_2 n_2 + \sum_{k=3}^{N} B_k n_k - \sum_{k=1}^{N-1} A_{k,1} n_k n_1$$

$$\dot{n}_j = B_{j+1} n_{j+1} - B_j n_j - \sum_{k=1}^{N-j} A_{k,j} n_k n_j + \frac{1}{2}\sum_{k=1}^{j-1} A_{k,j-k} n_k n_{j-k} \quad \text{for} \quad j = 2, ....., N-1$$

$$\dot{n}_N = -B_N n_N + \frac{1}{2}\sum_{k=1}^{N-1} A_{k,N-k} n_k n_{N-k} \qquad (4)$$

where the dot denotes time derivative, $B_j$ represents the fission rate of a cluster of mass $j$, defined by $B_j = (\widetilde{v}/R)\sqrt{j}$, and $A_{j,k}$ is the collision rate between clusters of mass $j$ and $k$, defined by $A_{j,k} = (\widetilde{v}\sigma_0/A)\left(\sqrt{j} + \sqrt{k}\right)$. $\sigma_0$ is the scattering cross section of a single rod. $R$ is the only free parameter and indicates the characteristic length a rod at the boundary of a cluster moves before it is leaving the cluster in a typical fission event. We assume $R = \alpha L$ taken into account that longer rods will stay attached to cluster for a longer time.

Since $\sigma_0$ can be approximated by $\sigma_0 \approx L + W = \sqrt{a}\left(\sqrt{\kappa} + \frac{1}{\sqrt{\kappa}}\right)$, the MFA depends only on the parameters $\kappa$, $a$, $A$, $\widetilde{v}$ and $\alpha$. If one integrates Eqs. (4) with parameters used in IBM simulations and an initial condition $n_j(t=0) = N\delta_{1,j}$, their solution yields steady state values $n_j^0$ for $t \to \infty$. From these values, we obtain a MFA for the weighted cluster size distribution $p(m) = n_m^0 m/N$ for given values of the free parameters $R$ resp. $\alpha$. The best agreement between the MFA and the IBM simulations is found for a choice of $\alpha = 1.0 \pm 0.05$ (see Fig. 3b). Hence, we will use $R = L$ in the following. To understand the relation between the parameters of the model and clustering effects, we can rescale Eqs. (4) by introducing a new time variable: $\tau = t\widetilde{v}/\sqrt{a\kappa}$. The resulting equations [15] depend only on a dimensionless parameter $P = (\kappa + 1)a/A$. Note that $\widetilde{v} \neq 0$ is scaled and does not affect the qualitative dynamics of the system. In the dimensionless model the parameter $P$ stands for ratio between fusion and fission processes and therefore triggers the transition from a unimodal to a bimodal cluster size distribution. We can easily establish a transition criterion, and by using a bisection method, we can accurately determine the critical transition parameter $P_c$. Given the system area $A$, the rod area $a$ and the number of rods $N$, this method provides a way to calculate $\kappa_c$:

$$\kappa_c = P_c(N)\frac{A}{a} - 1 \qquad (5)$$

At this point it is crucial that $P_c$ depends on $N$, which is formally the number of equations in the MFA. By numerically solving the MFA equations for different particle numbers $N$ up to $N = 1024$, we find $P_c(N) \propto N^{-1.026 \pm 0.023}$. This result indicates that in the MFA the critical parameter value $\kappa_c$ for the clustering transition does not depend on the number of particles. This does not imply that the weigthed distribution $p(m)$ is independent of $N$; in fact, we find that the probability for a rod to be in a large cluster increases with $N$. We proceed by assuming that $P_c$ is inversely proportional with

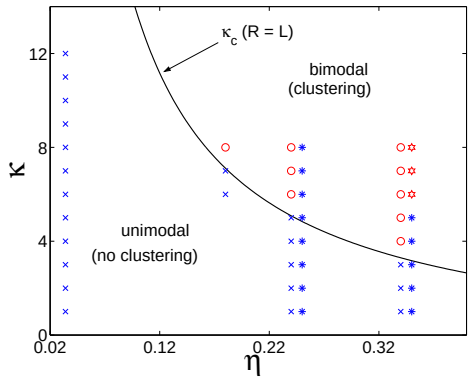


FIG. 4: $\kappa$-$\eta$ phase diagram. The solid line corresponds to the transition curve predicted by equation 6. The symbols indicate IBM simulations ($N = 100$). Crosses refer to unimodal $p(m)$ and circles to bimodal $p(m)$ of active particles. Stars refer to unimodal $p(m)$ and hexagrams to bimodal $p(m)$ of active-Brownian particles (color online).

$N$, we can express $\kappa_c$ as a simple function of the packing fraction:

$$\kappa_c = C/\eta - 1 \tag{6}$$

where the constant is found to be $C \approx 1.46$. The $\kappa$-$\eta$ phase diagram (Fig. 4) shows a reasonable agreement of the transition line given by Eq. (6) and the IBM simulation results. So, for the range of parameters used in the IBM, we retrieve in the MFA the unimodal shape of the weighted cluster size distribution for small values of $\kappa$ and $\eta$, and the bimodal shape for large values of the two parameters. Fig.3b gives a comparison of the cluster size distribution in the IBM and MFA.

In summary, we have found non-equilibrium clustering for interacting self-propelled rod shaped-particles with sufficient packing density $\eta$ and aspect ratio $\kappa$ in simulations. The rods interact via strong short range repulsive interactions that approximate excluded volume interactions. The onset of clustering has been defined by a transition from a unimodal to bimodal cluster size distribution. This transition is reproduced by a mean-field description of the cluster size distribution, which yielded a simple criterion, $\kappa = C/\eta - 1$, for the onset of clustering. This functional form with $C \approx 1.46$ provides a good fit to the results of the simulations. The high density inside the cluster leads also to alignment of rods and coordinated motion of all particles in the cluster. The transition to clustering defined here is practically independent of the system size resp. the number of particles. It is instructive to compare our result rewritten in the form $\kappa\eta + \eta \approx 1.46$ with the formula for the isotropic-nematic transition $\kappa\eta \approx 4.7$ found in the two-dimensional version [16] of Onsagers mean-field theory for Brownian rods [9]. This shows that actively moving rods can achieve alignment at much lower densities than Brownian rods resp. particles in equilibrium systems. The clustering phenomenon is absent in simulations with isotropic self-propelled particles as well as with Brownian rods. Our model provides also an alternative explanation for collective behavior of rod-shaped objects - previous swarming models have achieved aggregation and clustering by assuming attractive long-range interactions [4, 5]. With respect to biology, our observation offers a simple physical explanation for the formation of clusters in many gliding rod-shaped bacteria, that often precedes the formation of biofilms and the appearance of more complex patterns. **Acknowledgement:** We acknowledge financial support of Deutsche Forschungsgemeinschaft (DFG) through grant DE842/2 and fruitful discussions with L. Morelli, L. Brusch, J. Starruss and L. Sogaard-Andersen.

[1] D. Helbing, Rev. Mod. Phys. **73**, 1067 (2001); F. Schweitzer, *Brownian Agents and Active Particles*, (Springer, Berlin, 2003); J. Toner *et al.*, Ann. Phys. (N.Y.) **318**, 170 (2005).
[2] E. Ben-Jacob *et al.*, Adv. Phys. **49**, 395 (2000).
[3] I. H. Riedel *et al.*, Science **309**, 300 (2005).
[4] T. Vicsek *et al.*, Phys. Rev. Lett. **75**, 1226 (1995); G. Gregoire and H. Chate, Phys. Rev. Lett. **92**, 25702 (2004).
[5] U. Erdmann *et al.*, Eur. J. Phys. B **15**, 105 (2000); Phys. Rev. E **71**, 051804 (2005).
[6] (a) *Myxobacteria II*, M. Dworkin and D. Kaiser (Eds.),(American Society for Microbiology, Washington DC, 1993); (b) D. Kaiser, Nat. Rev. Microbiol. **1**, 45 (2003); (c) L. Jelsbak and L. Sogaard-Andersen, Proc. Natl. Acad. Sci. USA **99**, 2032 (2002).
[7] D. Dusenbery, Proc. Natl. Acad. Sci U.S.A. **94**, 10949 (1997).
[8] R. Kemkemer *et al.*, Eur. Phys. J. E **3**, 101 (2000).
[9] L. Onsager, Ann. N. Y. Acad. Sci. **51**, 627 (1949).
[10] (a) H. Reichenbach, Ber. Deutsch. Bot. Ges. **78**, 102 (1965); (b) Myxobacteriales: Schwarmentfaltung und Bildung von Protocysten, Institut für den wissenschaftlichen Film, Göttingen, 1966.
[11] U. Börner *et al.*, Phys. Rev. Lett. **89**, 78101 (2002).
[12] M.S. Alber *et al.*, Phys. Rev. Lett. **93**, 68102 (2004); O. Igoshin *et al.*, Proc. Natl. Acad. Sci. USA **101**, 4256 (2004).
[13] Parameters: $a = 0.2$, $1/\zeta_\parallel = 0.1$, $1/\zeta_\perp = 0.04$, $1/\zeta_\theta = 0.5$, $F = 0.4$, $\gamma = 0.16$, $\phi = 1.96$, and $\beta = 1$. Additive white noise terms: $\overline{R_\parallel^2}/\zeta_\parallel = \overline{R_\perp^2}/\zeta_\perp = \overline{R_\theta^2}/\zeta_\theta = 0.0833$ for active-Brownian particles. Simulations were performed with $N = 50$, 100 and 200, and simulation times $10^4$ in discrete steps $\delta t = 0.1$.
[14] S. Chandrasekhar, Rev. Mod. Phys. **15**, p. 59 ff (1943).
[15] $\dot{n}_j = \sqrt{j+1}n_{j+1} - \sqrt{j}n_j + P[\frac{1}{2}\sum_{k=1}^{j-1}(\sqrt{k} + \sqrt{j-k})n_k n_{j-k} - \sum_{k=1}^{N-j}(\sqrt{j} + \sqrt{k})n_k n_j]$ for $j = 2, ..., N-1$.
[16] R. F. Kayser and J. Raveche, Phys. Rev. A **17**, 2067 (1978).